 Wolfgang Predki, Dietmar Vill, Jennifer Papies, Chair of Mechanical Components and Power Transmission, Ruhr University Bochum

Multi-Body Simulation of a Planetary Gearing Test Bench

RUHR UNIVERSITÄT BOCHUM RUB

LMGK Lehrstuhl für Maschinenelemente, Getriebe und Kraftfahrzeuge Prof. Dr.-Ing. W. Predki

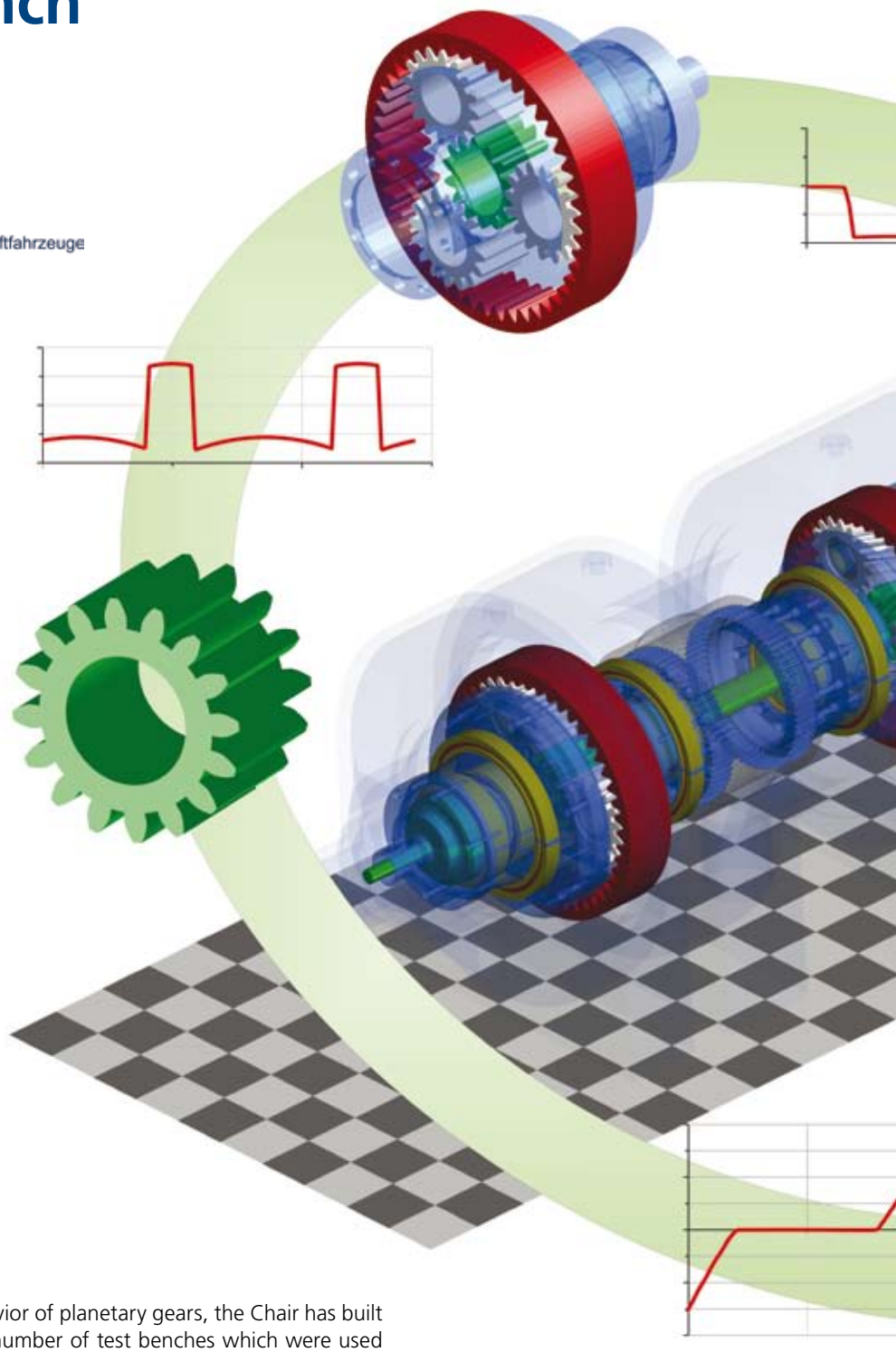

The Chair of Mechanical Components and Power Transmission at Ruhr University of Bochum (LMGK) researches a wide range of machine components. Besides spur gears, further research focuses on worm and planetary gears as well as bearings. These fields of research are investigated on experimental and theoretical levels.
Motivated by the question of how the effect of the interaction between planetary gear stages can be characterized, this article explores whether the resulting noise level can be influenced by the choice of meshing sequence. Theoretical conclusions are compared with experimental results in order to prove whether the level of noise emanating from gear interaction can be predicted and reduced with the help of simulations. In addition, this article deals with the analysis of the dynamic behavior of bearings, describing the simulation of cylindrical roller bearings and introduces a pilot study on the implementation of ball bearings.

INTRODUCTION

Due to the increasing demands on power trains in the wind power and automotive industries, planetary gears are used more frequently. This is partly due to their coaxial, and thus, space saving design. Secondly, because of their torque division, they have an especially high power density and, in general, good efficiencies. To single out these advantageous properties and their behavior within the entire drive train, effective simulation programs have become available. Especially in the investigation of multi-body dynamics of planetary gears, LMGK looks back on many years of experience from theoretical and experimental points of view. To analyze the dynamic behavior of planetary gears, the Chair has built a number of test benches which were used in various research projects. One of these existing back-to-back planetary gearing test benches (center distance of 100 mm) is represented and simulated within SIMPACK. In this investigation, the influence of different contact mesh sequences on the dynamics of the total system has been analyzed. In order to evaluate the simulation results they were compared with test bench data and results, from the Chair´s own simulation program from a previous project [5].

"...FE225 enables the fluctuating tooth stiffness, which is indispensable in analyzing the different contact mesh sequences."

In planetary gears, the chronology of the meshing of the teeth involved depends

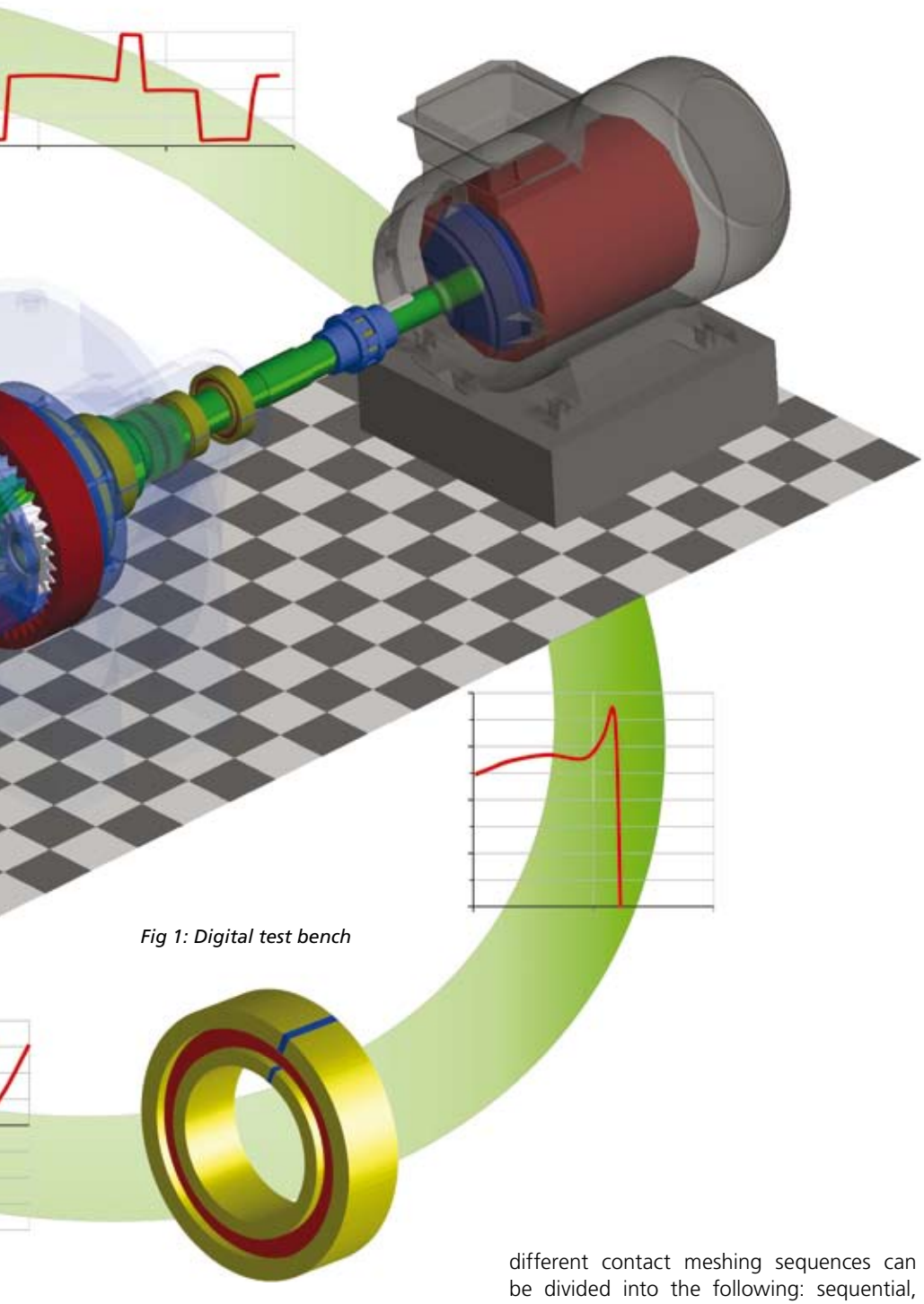

Fig 1: Digital test bench

only on the macro-geometry of the gears, namely the number of teeth and the angular pitch of the planet carrier. The interaction between these meshing teeth provides an additional parameter for excitation because of their phase delayed stiffnesses. Here, the different contact meshing sequences can be divided into the following: sequential, symmetric and unbalanced.

TEST BENCH

The test bench mentioned above has a back-to-back design, two planetary gear boxes that are directly connected to each other. For this purpose, tooth couplings are used to connect the sun shafts and planet carriers respectively, which also allows for compensation of any possible axial, radial and angular shaft misalignment. The transmission gear box is located on the motor facing side. By interlocking the central elements, a circulating mechanical power is achieved. By turning the ring gear of the transmission gear box, the load level of the test gear box can be adjusted. This design offers the advantage that the engine only has to compensate for the power dissipation in the system, which represents only a fractional amount of the whole circular power. The coupling shaft between the two sun gears also functions as a gauge bar providing an electrical signal in proportional relation to the torque setting. In both the test gear box and the transmission gear box, sun shafts are embedded by tapered roller bearings to absorb any arising axial forces by using helical test gears. The outer rings of the transmission gear sun shafts are attached to the housing. A schematic representation is shown in Fig. 2.

DIFFERENT TEST BENCH CONFIGURATIONS

Twelve different test bench configurations are analyzed with respect to their excitation behavior. Due to the requirement of the kinematic equality of both gear boxes, it is also necessary to vary the transmission gear box configuration. The design parameters of the test gears have been chosen to allow a combination of several test gear boxes with one transmission gear unit.

MODEL DESCRIPTION

The SIMPACK model of the test bench [1] consists of several subsystems which are representative of the real test bench components and allow the analysis of the different configurations. The model provides a true representation of sun shafts broken down into their various sections for which the respective stiffnesses and mass properties are estimated by means of established calculation methods. The individual results are added together using bushing elements to arrive at a realistic model of the real deflection of the sun shaft in reaction to torsional and bending loads. The necessary grade of discretization is verified by FEM.

For modeling of involute gear contacts, SIMPACK dedicated Force Element FE225 is used within the model. This element enables the fluctuating tooth stiffness which is indispensable in analyzing the different contact mesh sequences. To improve the calculated stiffness, the parameterization of FE225

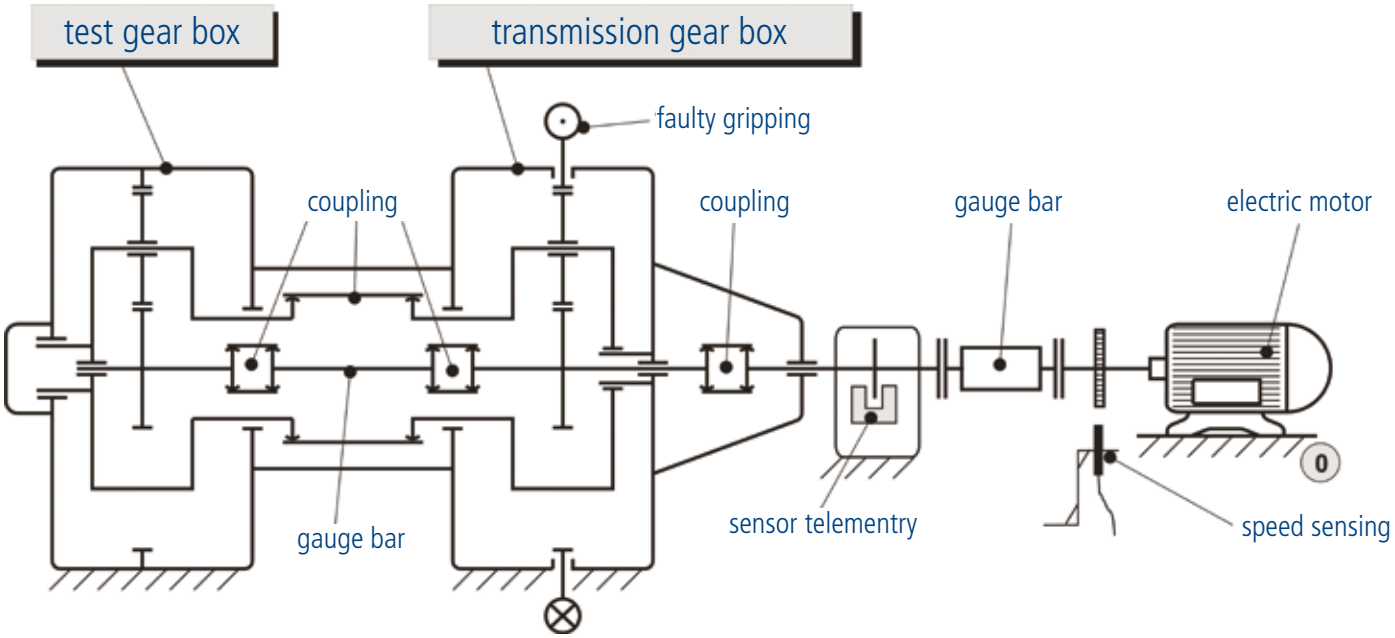

Fig 2: Schematic diagram of the test bench

can be changed until it corresponds to a solution derived from an approximate equation from previous projects. All gears are regarded as free of deviation within this model. The electric motor is represented by its torque-drive characteristic which is included by Expressions in the program.
All couplings are only represented by their stiffness characteristics. To take account of the stiffness behavior of bearings, which is dependent on the loading condition, bearings including a non-linear characteristic and clearance are used within the model. Subsequently, the stiffness is then considered with the help of Input Functions.

"...bearings including a non-linear characteristic and clearance are used..."

SETTINGS FOR THE SIMULATION RUNS

For the calculation of the different levels of the several variants these were, with few exceptions, always averaged over a speed range of 0 rpm to 2.500 rpm. Due to the high computing time and the resulting amount of data, a continuous determination of the level values of certain variables is not possible. An average determination is made over five stationary operating points at different speeds for comparism to experimental results. Since the start-up procedure to a steady state system status makes up a substantial part of the computing time, the system is first accelerated to 2.500 rpm. The system is then decelerated as shown in Fig. 4. The rotational position of the planet carrier is also plotted in this diagram. The length of time in which an operating point must be considered is determined by the rotational speed of the planet carrier. The figure shows that, in each case, one planet carrier rotation is captured. The specified measurement rates are based on the Nyquist-Shannon sampling theorem.

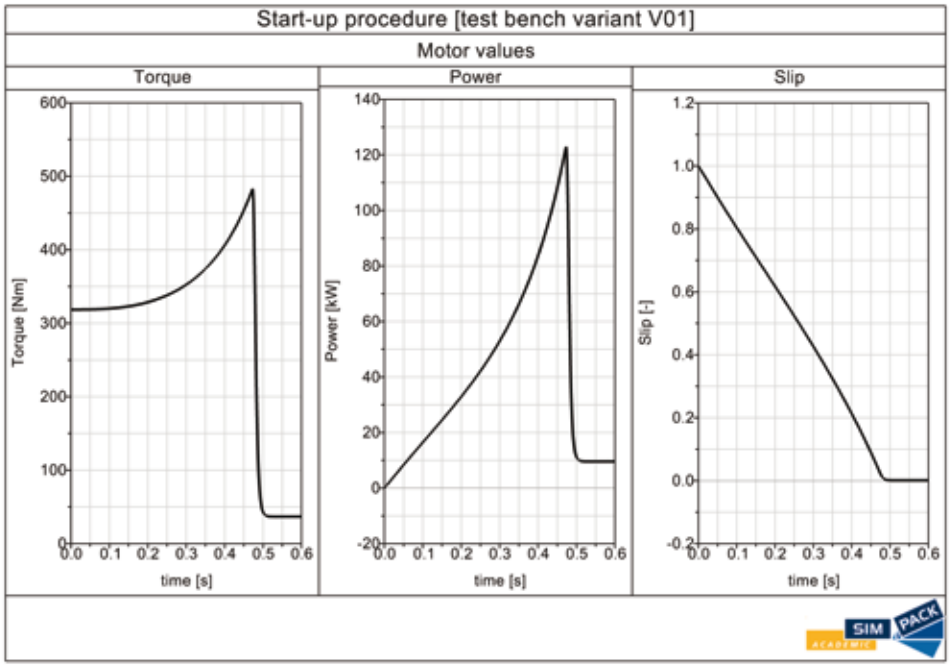

Fig 3: Start-up procedure

SIMULATION RESULTS

The comparison between the measurements gained and the simulation show qualitatively similar results. Given symmetric contact mesh sequences, the central elements hardly ever misalign. In sequential variants, the behavior is rather periodic, and in unbalanced mesh sequences, the characteristic proves to be chaotic (Fig. 5). The behavior of unbalanced variants can be attributed to a predominant power imbalance which moves the central elements out of their central points.
Therefore, symmetric variants show a significantly lower level of displacement to unbalanced ones. This is shown in Figures 6 and 7.

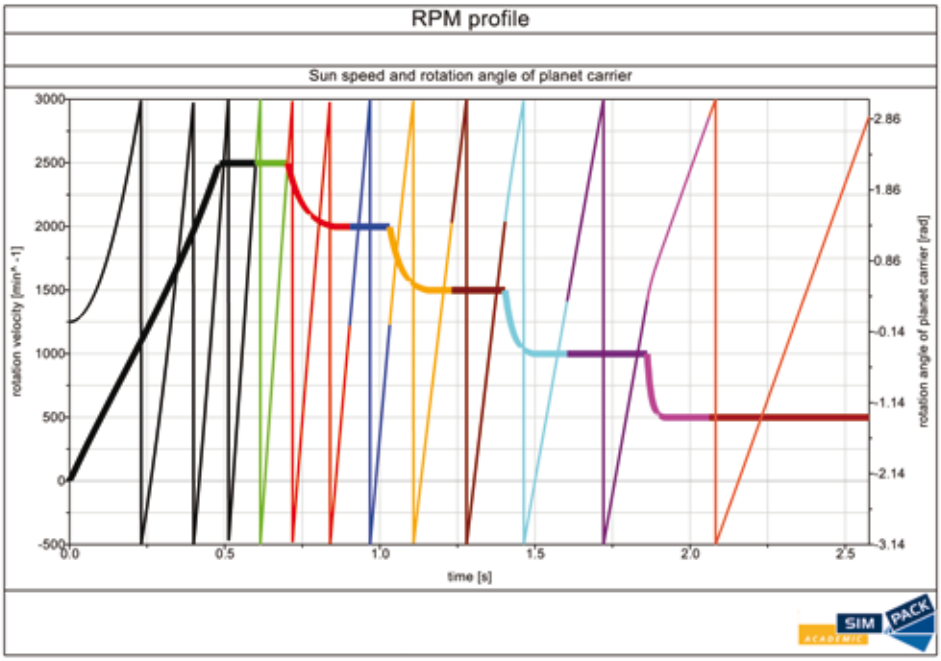

Fig 4: RPM profile

By contrast, the speed level presents an inverse attitude (Fig. 8). The meshing itself can be identified as a decisive parameter for the excitation of the system. Compared to sequential types, variants with a symmetric mesh sequence show, a significantly less favorable behavior in regard to their displacement excitation. This is justified by the permanent change of stiffness levels which occur in distinctive steps caused by symmetric variants. Here, sequential variants with four planets turned out to be particularly balanced.

The absolute tooth force level L_{Fz} characterizes the vibration excitation of gearings [2]. This parameter unites all essential constituents of the vibration excitation and can be correlated with the emitted airborne noise. Fig. 9 shows the absolute tooth force level as well as the measured sum acceleration level on the ring gear of the test gear box.

FUTURE WORK

To improve the quality of these current models, and to take other important influences into account, these models are being further developed. The consideration of gearing deviations and tolerances play an especially important role on the system dynamics and is treated in current projects. However, gearing deviations only cause an appreciable inhomogeneity on the load distribution of the different tooth engagements in planetary gears if all central elements are firmly embedded, i.e., no compensatory adjustment movements are possible. To capture this within the simulations, two different approaches are pursued. On one hand, representative normalized functions for the acting excitation of the gearing deviations are imported into SIMPACK Expressions and are used in the model from then on. However, this solution is quite complex. Therefore, on the other hand, SIMPACK User elements are used in which these functions are calculated. Both solutions work in test models (Fig. 10), but must be included and tested in the overall model of the test bench.

"...the influence of the planet carrier deformation should be considered..."

Simultaneously, calculations of load distributions are performed, and the influence of the planet carrier deformation should be considered within this model.

FURTHER APPLICATIONS

In addition to the overall dynamic of drive train systems, the department is dealing with the dynamic behavior of their subcomponents, for example, bearings. A typical application of cylindrical roller bearings is, due to their high load carrying capacity and their compact design, on the output stage of spur or planetary gear boxes. At this point, because of the permanently increasing power density, very high loads occur at low speeds so that the requirement rises in accordance with these components.

The simulation of the slow-speed abrasive wear of cylindrical roller bearings is based on a research project [3] within the department. The lubrication oil film is not considered in this model; only boundary friction exists. This assumption is legitimate because the lubrication oil film does not form at low speed. The inner ring is loaded by a constant dead weight with large mass; the outer ring is fixed.

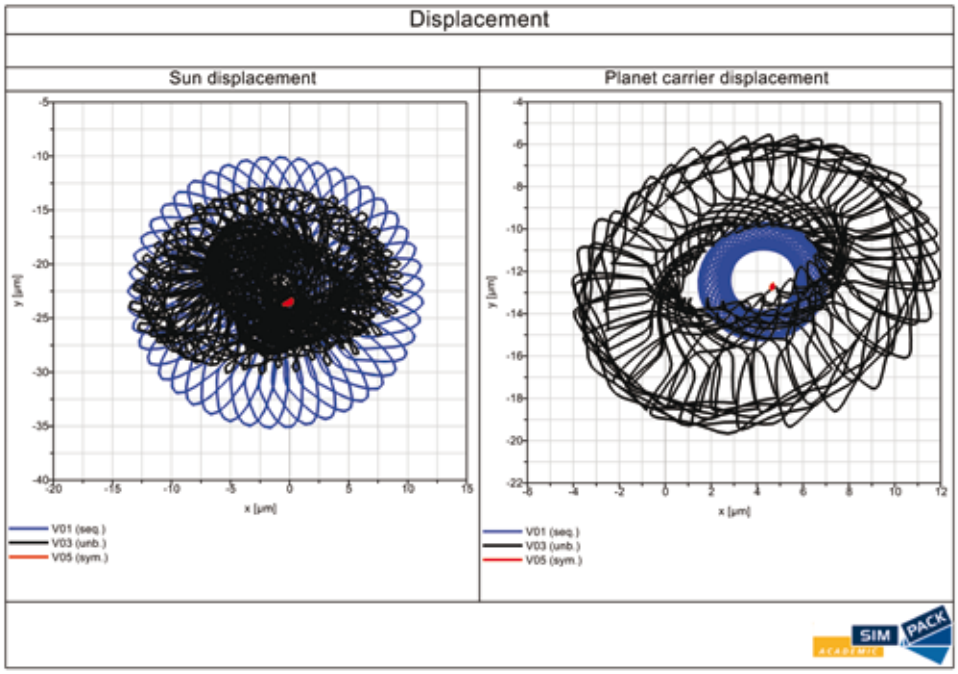

Fig 5: Sun and planet carrier displacement

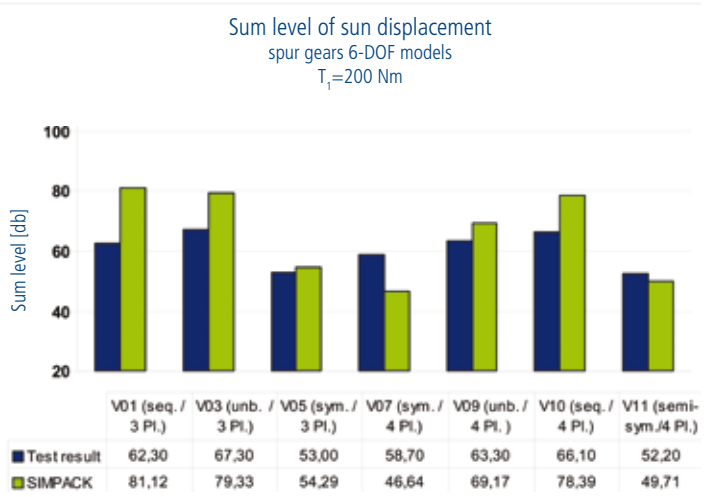

Fig 6: Sum level of sun displacement

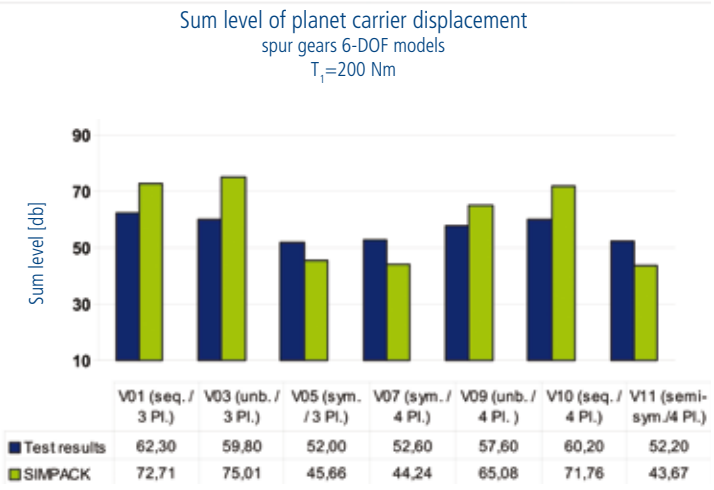

Fig 7: Sum level of planet carrier displacement

PILOT STUDY: Cylindrical Roller Bearing Under Loads Within A Planetary Gear Stage

The model parameters differ from those of [4]. This allows only a qualitative comparison of the results. It can be concluded that the friction of planetary gear bearings is much higher than in non-portable bearings.

The increase of the angular velocity before entering the load zone can clearly be explained by the fact that the roller element installed before the one under observation, which can rotate freely, is already gripped by the load zone. The following roller element, which is attached to the one before, is turned with increasing speed in the opposite direction until it enters the load zone itself.

PILOT STUDY: Ball Bearing

In general, ball bearings can absorb radial and axial forces in both directions. However, they can absorb much greater forces in the radial direction. This property can be attributed to their raceway geometry and their ball-shaped rolling elements. However, the osculation of the rolling elements and the raceways gives it the ability to carry loads. Similar to the roller bearing, the outer ring is considered to be fixed. In contrast, the inner ring is provided with six degrees of freedom. Finally, it should be able to reduce and rotate in direct reaction to the load. In addition, the modeling of the raceways forms another challenge. This was solved by the approximation of the contact ellipse through several point-to-point contacts. To guarantee a correct bearing deflection, the e-modulus within the Force Element was adjusted. The deflection characteristic was given by the manufacturer. The bearing is designed with clearance. The contact between the rolling elements and their housing is described by the Hertzian contact. For this purpose, within the model, the cage pockets themselves are represented as spheres and are positioned inside the rolling elements. The rolling elements are designed as spheres as well. All contacts are modeled with the help of the Hertzian contact Force Element FE222. Some simulation results are shown in Fig. 13.

The angular velocity of the roller elements shows an expected pattern. The rotational velocity changes during the passage through the load zone. Even the circular course of the increase and the decrease of speed is recognizable. This effect is based on the deformation of the rolling element within the load zone. The radius minimizes continuously from the time of the arrival at the load zone to the crown of the ball position. From this point it decreases until the roller element resurges in the load zone. A more detailed view of the angular velocity of the housing shows fluctuation from the calculated value. The reason for this is the movement of the roller elements since, they both push and slow down the cage pocket. Additionally, the slip velocity of one roller element is shown in Fig. 13. Due to the

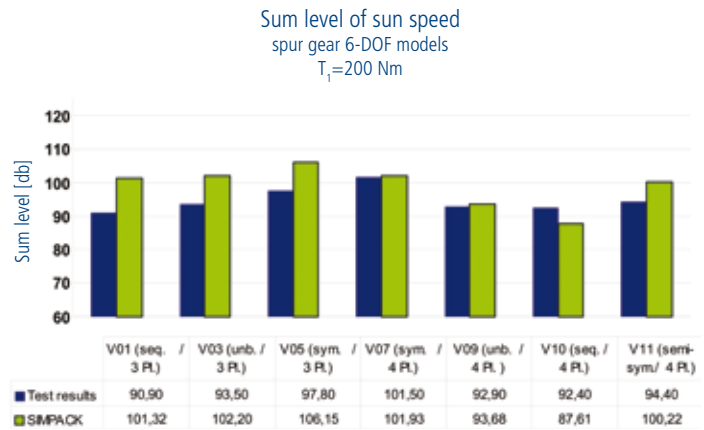

Fig 8: Sum level of sun speed

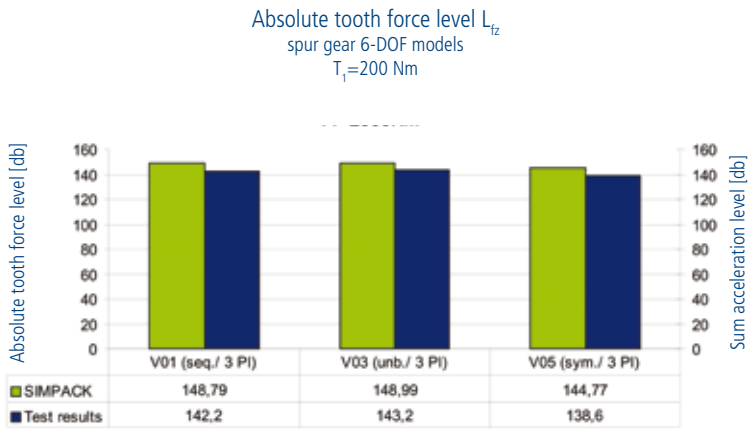

Fig 9: Absolute tooth force level

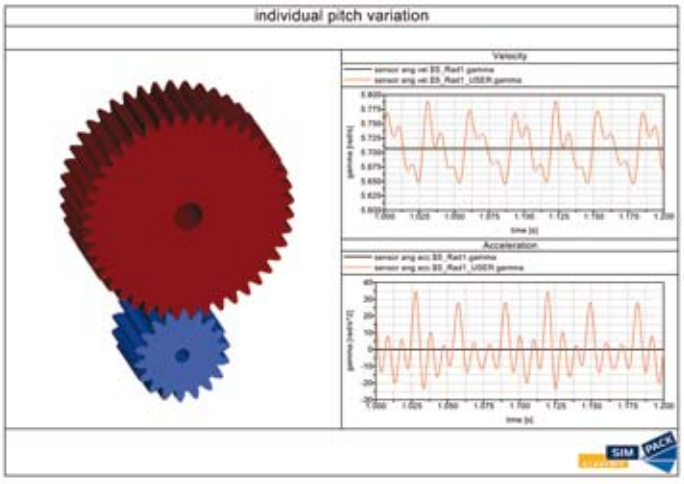

Fig 10: Individual pitch variation

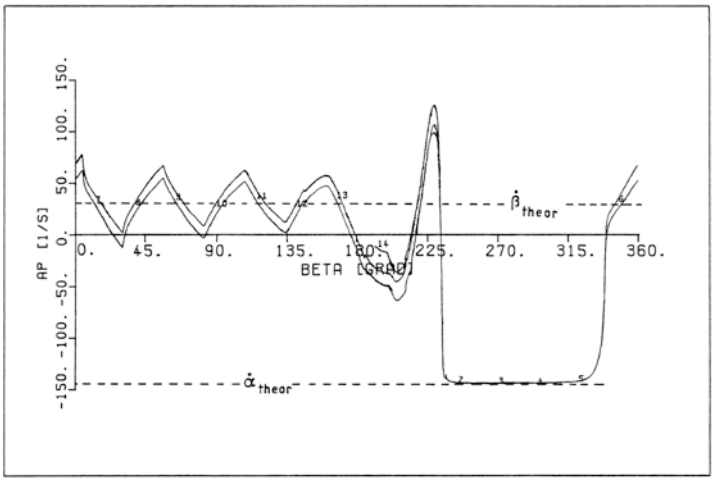

Fig 11: Roll angular velocity [4]

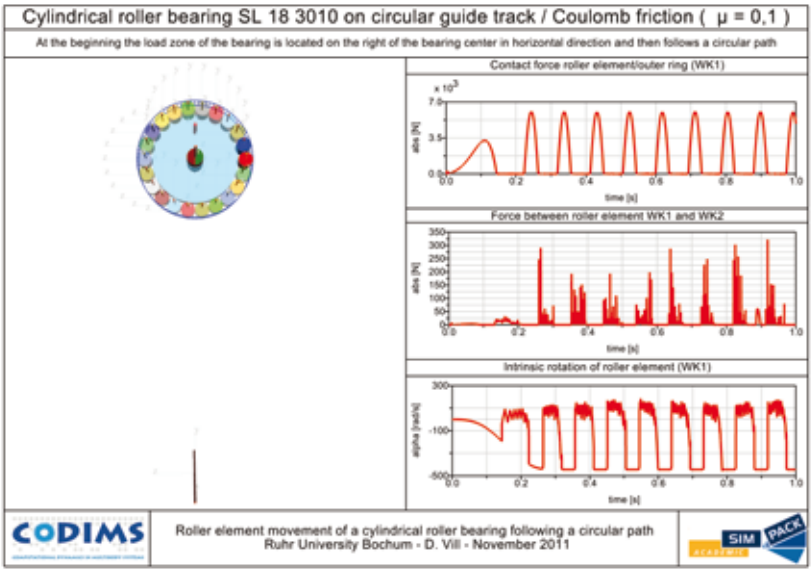

Fig 12: Cylindrical roller bearing SL 18 3010

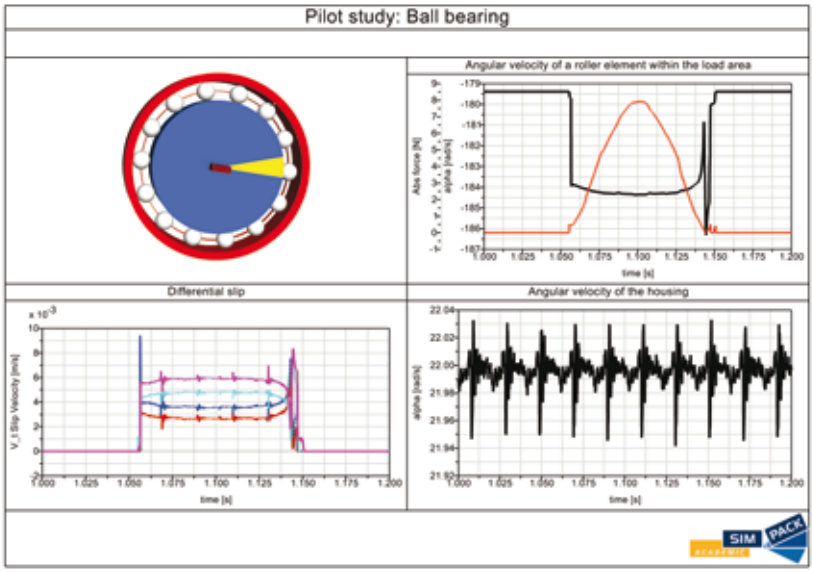

Fig 13: Ball bearing

geometry and the driven inner ring, the roller element has a higher slip velocity on the inner ring. The roller element has no angular velocity once it has reached the load zone. The slip velocity then reaches its maximum due to the high speed difference.

REFERENCES

[1] Feller, H.: Systemdynamik eines Planetengetriebeverspannungsprüfstands, Ruhr-Universität Bochum, Unveröffentlichte Bachelorarbeit, 2011

[2] Müller, R: Schwingungs- und Geräuschanregung bei Stirnradgetrieben, Dissertation, TU München, 1991

[3] Elfert, G.: Langsamlaufverschleiß von vollrolligen Radialzylinderrollenlagern, Dissertation, Ruhr-Universität Bochum, 2005

[4] Potthoff, H.: Anwendungsgrenzen vollrolliger Planetenrad-Wälzlager, Dissertation, Ruhr-Universität Bochum, 1986

[5] Sfar, M.: Bestimmung von Verzahnungskorrekturen und Lagerkräften in Planetengetrieben für Lastkollektive, FVA 328 IV Plankorr, Bochum, 2011